MDPI

Article

Regularities of Friction Stir Processing Hardening of Aluminum Alloy Products Made by Wire-Feed Electron Beam Additive Manufacturing

Tatiana Kalashnikova *, Andrey Chumaevskii, Kirill Kalashnikov [ID], Evgeny Knyazhev, Denis Gurianov [ID], Alexander Panfilov, Sergey Nikonov, Valery Rubtsov and Evgeny Kolubaev

Institute of Strength Physics and Materials Science, Siberian Branch, Russian Academy of Sciences, 634055 Tomsk, Russia; tch7av@gmail.com (A.C.); kkn@ispms.tsc.ru (K.K.); clothoid@ispms.tsc.ru (E.K.); desa-93@mail.ru (D.G.); alexpl@ispms.tsc.ru (A.P.); sergrff@ngs.ru (S.N.); rvy@ispms.ru (V.R.); eak@ispms.ru (E.K.)

* Correspondence: gelombang@ispms.tsc.ru

Abstract: Friction stir processing of additive workpieces in the sample growth direction (the vertical direction) and the layer deposition direction (the horizontal one) was carried out. The hardening regularities of aluminum-silicon alloy A04130 and aluminum-magnesium alloy AA5056 manufactured by electron beam additive technology were studied. For each material, 1 to 4 subsequent tool passes were performed in both cases. It was found that the formation of the stir zone macro-structure does not significantly change with the processing direction relative to the layer deposition direction in additive manufacturing. The average grain size in the stir zone after the fourth pass for AA5056 alloy in the horizontal direction was 2.5 ± 0.8 µm, for the vertical one, 1.6 ± 0.5 µm. While for the alloy A04130, the grain size was 2.6 ± 1.0 µm and 1.8 ± 0.7 for the horizontal and vertical directions, respectively. The fine-grained metal of the stir zone for each alloy in different directions had higher microhardness values than the base metal. The tensile strength of the processed metal was significantly higher than that of the additively manufactured material of the corresponding alloy. The number of tool passes along the processing line is different for the two selected alloys. The second, third and fourth passes have the most significant effect on the mechanical properties of the aluminum-magnesium alloy.

Keywords: friction stir processing; electron beam additive manufacturing; aluminum alloys; microhardness; microstructure; mechanical properties

1. Introduction

Aluminum-silicon alloy A04130 and aluminum-magnesium alloy AA5056 are structural materials widely used in the aircraft, spacecraft, vehicle and marine industries [1,2]. Since these industries are constantly developing, introducing advanced technologies into the manufacturing process of such enterprises is always a critical task. One of the most promising technologies from this point of view is electron beam additive manufacturing (EBAM) of large-sized products, which is based on the principle of metal wire melting in a molten pool. This method is very effective in producing high-quality components of different materials: titanium alloys [3,4], steels [5], copper alloys [6], aluminum alloys [7,8] and bimetallic products [9]. However, the products fabricated by the additive manufacturing method often require additional treatments to improve the structure and mechanical properties.

One of the methods of hardening metals is friction stir processing (FSP), which emerged from friction stir welding [10,11]. This method allows the hardening of metals and alloys by forming an ultrafine grain structure. When processing aluminum alloys, quite positive results were obtained [12], including, after EBAM [13], with an increase in the tensile strength and yield strength but a decrease in ductility. Most often, to achieve

satisfactory results, FSP is done in several passes [14], also in different directions [15]. As a result of FSP, the structure of metals significantly changes relative to the base metal, which is the main factor affecting the mechanical characteristics [16].

Positive factors of friction stir processing application are the increase of strength characteristics of materials, formation of ultrafine grain structure and the possibility of producing materials with composite structure [17]. It is essential in producing components with initially low strength properties, for example, produced by methods of high-performance additive manufacturing. The problem of producing EBAM samples from two fundamentally different alloys, aluminum-silicon casting alloy A04130 and aluminum-magnesium alloy AA5056, is forming a large-crystal softened structure. Such a situation leads to the necessity of additional processing after fabricating products for several applications, especially if high contact strength is required for the component operation. In this case, friction stir processing is the most appropriate. The friction stir processing can form composite materials on the product surface. It requires many tool passes to achieve a homogeneous strengthening phase distribution in the processed material surface layer [18]. In this regard, the research aimed at hardening these alloys after EBAM by FSP and identifying the effect of different numbers of passes on their mechanical characteristics.

2. Materials and Methods

Block-shaped samples sized $40 \times 40 \times 100$ mm^3 were produced at the self-developed wire-feed electron beam additive manufacturing equipment at the Institute of Strength Physics and Materials Science, Siberian Branch of the Russian Academy of Sciences, Tomsk, Russia. Parameters used for the manufacturing are showed in Table 1.

Table 1. Parameters of wire-feed electron beam additive manufacturing.

Alloy	Accelerating Voltage (kV)	Average Beam Current (mA)	Linear Printing Speed (mm/min)	Beam Sweep Shape	Beam Sweep Frequency (Hz)
A04130	30	45	400	Ring ∅5 mm	1000
AA5056	30	38.5	400	Ring ∅5 mm	1000

Next, the samples were cut into 3-mm-thick plates by electrical discharge machining. First, all the block's edges were cut off to achieve a parallelepiped, and then it was cut into equal-sized plates (Figure 1a). Then the plates of the as-built material were subjected to friction stir processing (FSP) on a laboratory stand for friction stir welding and processing. The FSP was performed on the samples in the growth direction (the vertical one) and in the layer deposition direction (the horizontal one), as shown in the scheme (Figure 1b). A 2.5-mm-high screw-pin tool with 12.5-mm-diameter shoulders was used for processing. The pin diameter is from 6.0 to 4.0 mm. For each material in both cases, processing was performed in 4 passes.

The process parameters for A04130 and AA5056 are shown in Tables 2 and 3. The process parameters were selected experimentally until a defect-free structure of the samples was achieved.

Table 2. Parameters of friction stir processing of A04130 alloy samples produced by electron beam additive technology. P—tool loading force, V—tool travel speed, ω—tool rotation speed.

No. of Sample	No. of Pass	Vertical			Horizontal		
		P (kg)	V (mm/min)	ω (rpm)	P (kg)	V (mm/min)	ω (rpm)
1.1	1	375	90	750	400	90	750
1.2	2	350	90	750	375	90	750
1.3	3	350	90	750	350	90	750
1.4	4	350	90	750	350	90	750
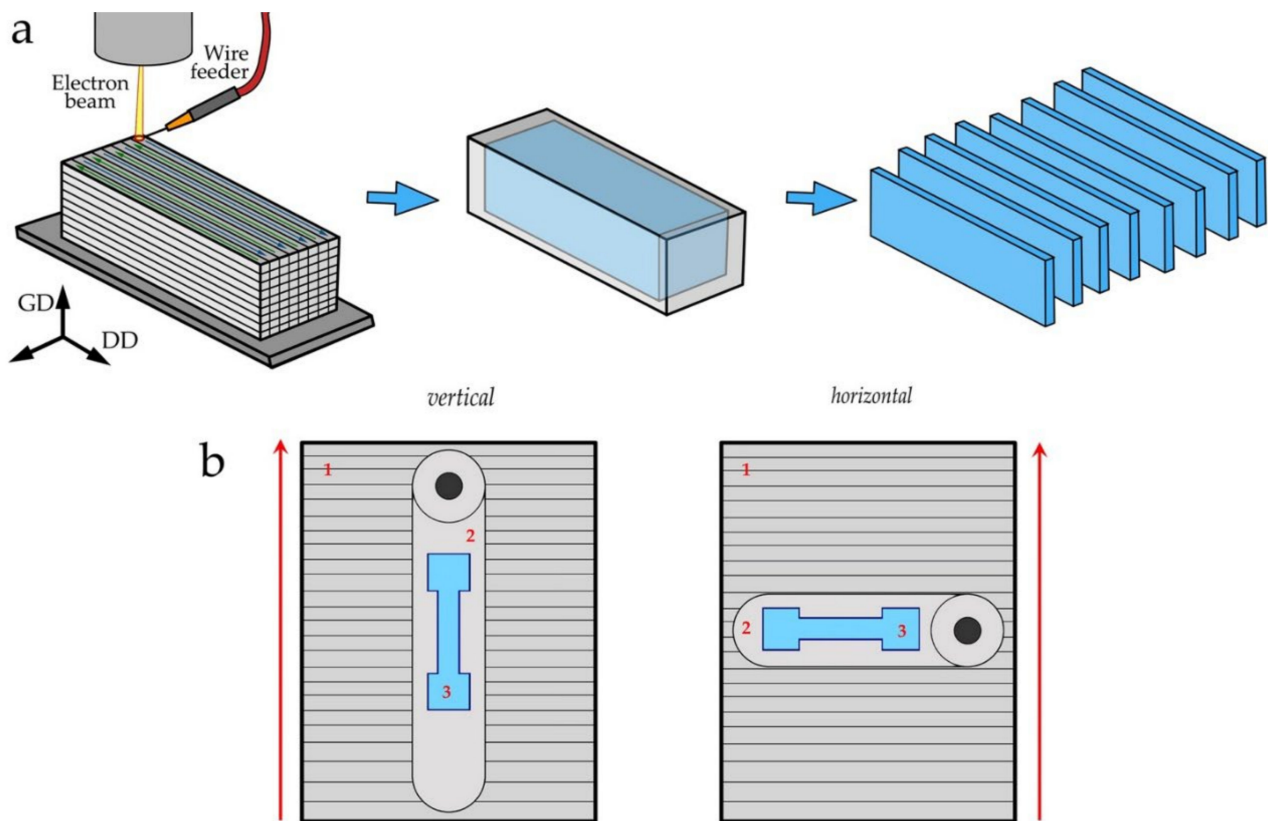
Figure 1. Wire-feed EBAM of block-shaped sample with subsequent cutting out of workpieces (**a**) and FSP in vertical and horizontal direction after wire-feed electron beam additive manufacturing (**b**). 1—EBAM'ed sample; 2—friction stir processing area; 3—scheme of specimen cutting out for uniaxial tensile tests; GD—sample growth direction, DD—layer deposition direction. The red arrow is the direction of sample growth in electron-beam additive manufacturing.

Table 3. Parameters of friction stir processing of AA5056 alloy samples produced by electron beam additive technology. P—tool loading force, V—tool travel speed, ω—tool rotation speed.

No. of Sample	No. of Pass	Vertical			Horizontal		
		P (kg)	V (mm/min)	ω (rpm)	P (kg)	V (mm/min)	ω (rpm)
2.1	1	900	90	500	900	90	500
2.2	2	850	90	500	850	90	500
2.3	3	800	90	500	800	90	500
2.4	4	750	90	500	800	90	500

The processing zone structure samples were cut using electrical discharge machining on an EDM-machine DK7745 (Suzhou Simos CNC Technology Co., Ltd. Suzhou, China) in a section perpendicular to the FSP direction. The samples were ground, polished, and etched to obtain metallographic images. The macrostructure was examined with an Altami MET 1T optical microscope (Altami Ltd., Saint Petersburg, Russia), and the microstructure with a JEOL JEM-2100 transmission electron microscope (TEM) (JEOL Ltd., Akishima, Japan). Thin foils for TEM studies were prepared in a section perpendicular to the FSP tool movement direction from the center of the stir zone. After that, they were mechanically ground, polished, and finalized by ion thinning-out.

Mechanical uniaxial tension tests were carried out on a universal testing machine "UTS 110M-100" (TestSystems, Ivanovo, Russia). The test specimens were cut along the

processing line (Figure 1) with the gauge length of 12 mm and 2.5 mm in width and thickness.

Microhardness measurements were carried out on a Duramin 5 microhardness tester (Struers A/S, Ballerup, Denmark) at a load of 490.6 mN (50 g), indenter time of 10 s. Microhardness profiles were obtained in the horizontal section from the base metal on the retreating side through the stir zone to the base metal on the advancing side.

3. Results and Discussion

3.1. Stir Zone Macrostructure

Optical macro-photographs of the structures after the FSP show that the stir zone, formed by the first tool pass, changes with each subsequent one. It is observed in both the vertical and horizontal directions of the FSP. Figure 2 shows the macrostructure of samples made by electron beam additive manufacturing from AA5056 alloy after FSP in the vertical and horizontal directions. By image contrast in the stir zone (SZ), due to the etching features, one can see that due to the small height of the tool containing only one spiral groove, the tool grabs and transfers a small amount of metal as a result of the adhesion interaction during the first pass. During subsequent passes, the SZ increases significantly as the tool mixes and transfers already recrystallized fine-grained material. During the first three passes, the SZ is represented by layers of different thicknesses and directions transferred by the tool. During the fourth pass, the literature changes into a characteristic structure called "onion rings" [19]. The macro-images of A04130 alloy samples (Figure 3) show a similar formation of the SZ from the first to the fourth pass. It is especially noticeable on the samples processed in the horizontal direction. The etching clearly shows banded layers of additive metal from the retreating side (RS), which deform visibly during subsequent passes and, as a result of structure fragmentation, are completely refined.
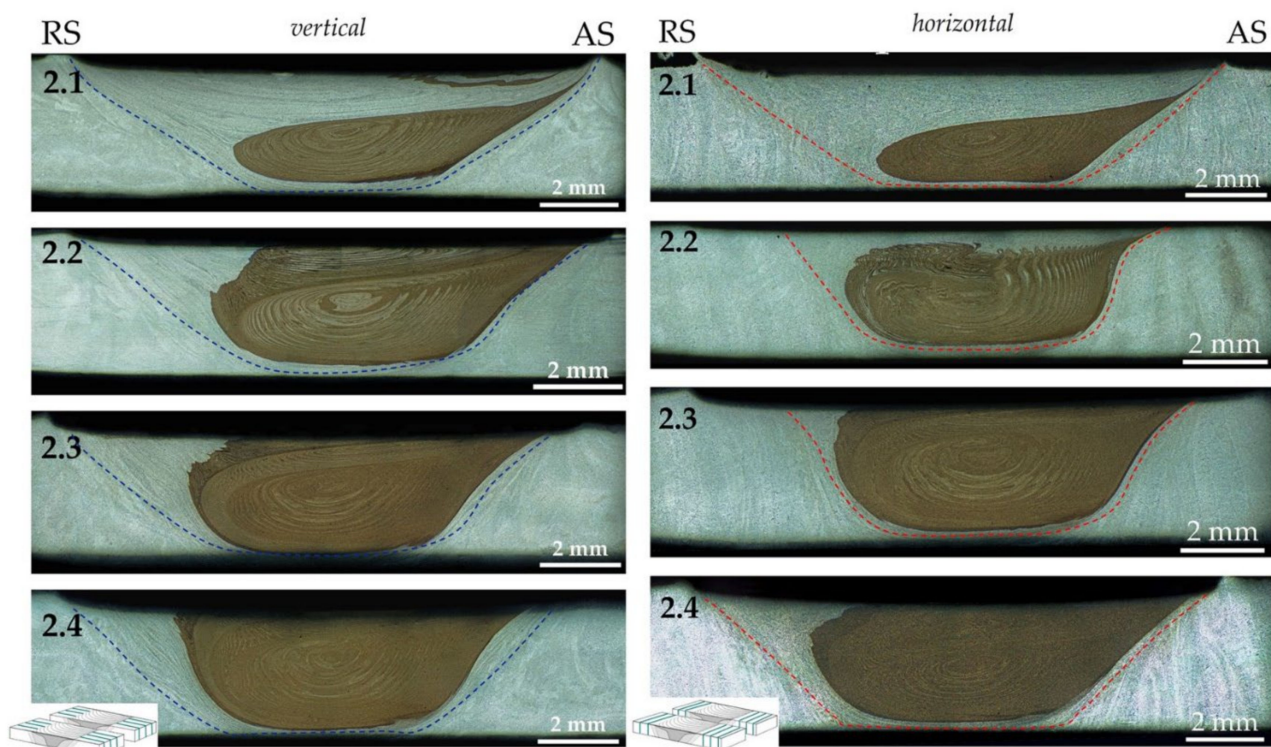

Figure 2. Macrostructure of samples made by electron beam additive technology from AA5056 alloy after FSP in vertical and horizontal direction by modes 2.1–2.4. RS—retreating side, AS—advancing side, blue and red dashed lines indicate the stir zone boundaries.
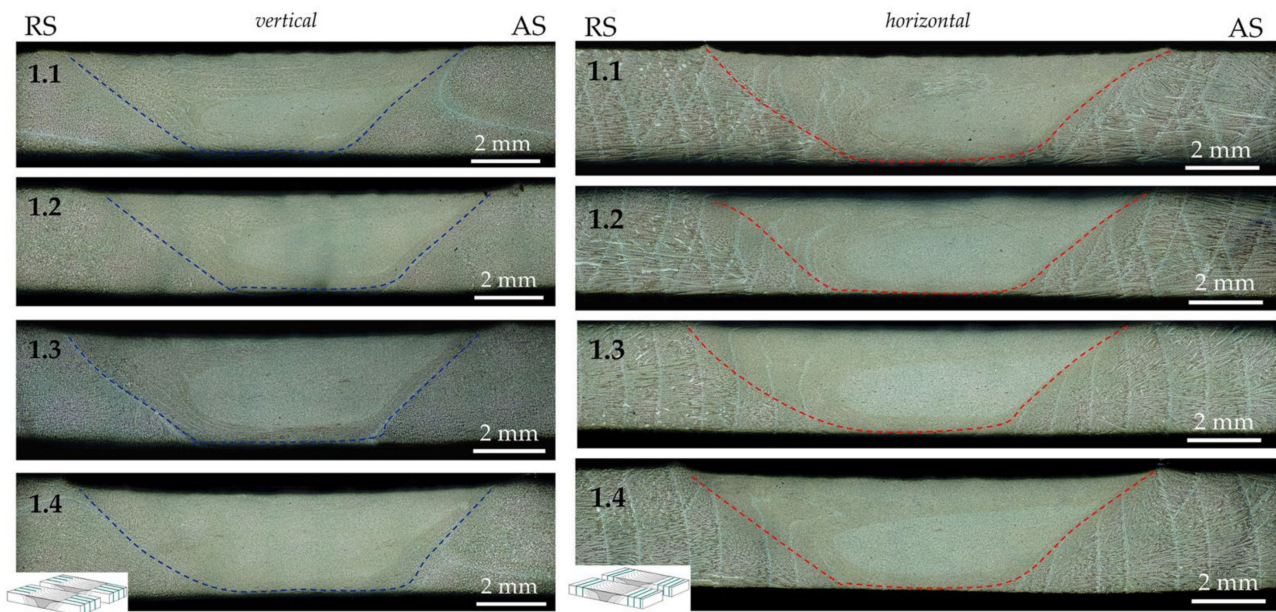
Figure 3. Macrostructure of EBAM samples made of A04130 alloy after FSP in vertical and horizontal direction by modes 1.1–1.4. RS—retreating side, AS—advancing side, blue and red dashed lines indicate the stir zone boundaries.

The base metal of AA5056 alloy after the EBAM process is represented by large elongated grains, which grow epitaxially. The average grain size varies from 132.5 μm and 76.1 μm to 52.7 μm and 30.4 μm in height and width, respectively (Figure 4a). In the samples made of the A04130 alloy, the base metal is represented by a dendritic structure whose direction coincides with the block-shaped sample growth direction. Dendrites predominantly grow within a single layer (Figure 4b).
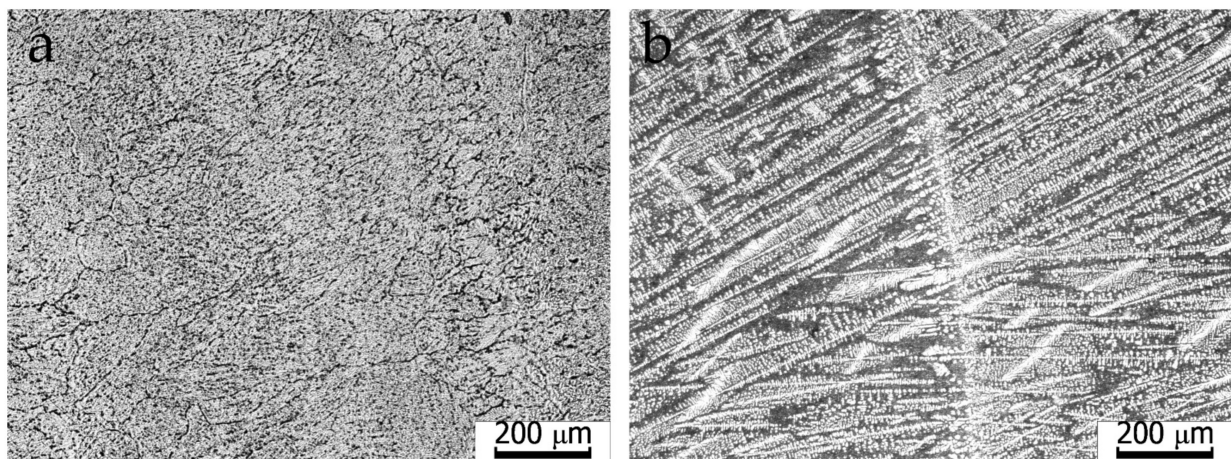

Figure 4. Base metal in as-built samples of AA5056 (**a**) and A04130 (**b**) after electron beam additive manufacturing.

As a result of grain refinement in the stir zone, it is impossible to analyze the structure in this area using an optical microscope Altami MET 1T. Therefore, studies were carried out using transmission electron microscopy. When analyzing the TEM images of AA5056 alloy samples, it was found that the microstructure is represented by dynamically recrystallized grains with chaotically distributed dislocations. After the fourth pass in the horizontal direction, grains with a shape close to equiaxial prevail, the average size of which is 2.5 ± 0.7 μm, while in the vertical direction, grains are refined to 1.6 ± 0.5 μm (Figure 5a,b).
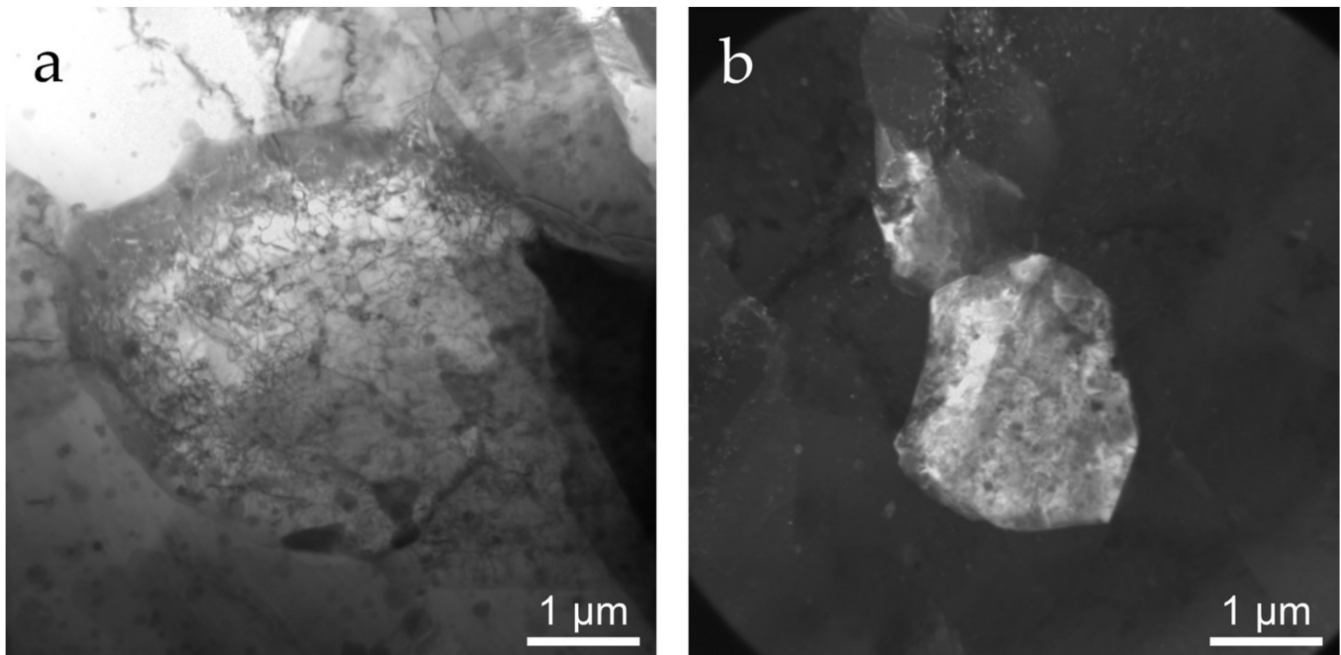
Figure 5. TEM images of grains and dislocation loops in the stir zone of AA5056 alloy samples after the fourth pass in the horizontal (**a**) and vertical (**b**) directions.

In the samples from alloy A04130, one can observe that initially, the structure is represented by dendrites, but after FSP forms grains with an average size of 2.6 ± 1.0 μm when processed horizontally (Figure 6) and 1.8 ± 0.7 in the vertical direction (Figure 7). At the same time, the morphology of the grain structure has apparent differences. When processed horizontally, a predominantly equiaxed structure is formed, whereas, in the vertical direction, the grains have an elongated shape. Moreover, in the vertical direction, the size of some grains is close to the nanoscale (Figure 6).
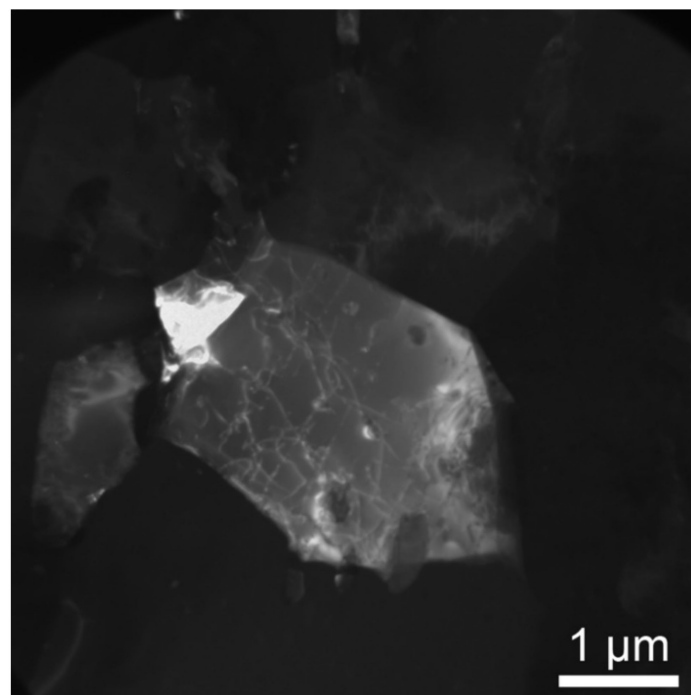
Figure 6. TEM image of the grain structure in the stir zone of the A04130 alloy sample after the fourth pass in the horizontal direction.
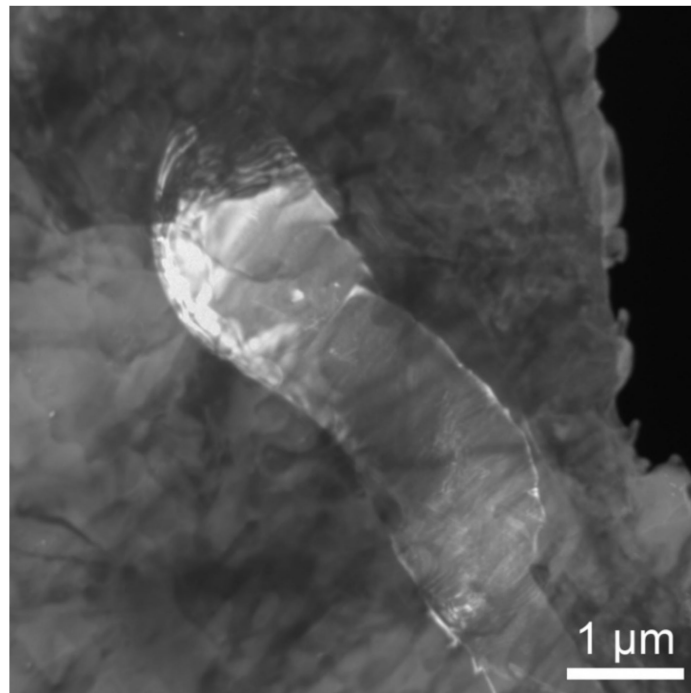
Figure 7. TEM image of the grain structure in the stir zone of the A04130 alloy sample after the fourth pass in the vertical direction.

Presumably, this position is caused by the fact that when the tool moves along the processing line during the initial stages of the FSP process, vertically elongated grains or dendrites are more amenable to fragmentation and refinement than those located across the tool movement line. In this case, the tool travel along elongated grains or dendrites can cause more significant damage to the original structure, as observed in this study.

3.2. Mechanical Properties

In tensile tests of electron beam additive manufacturing samples of alloy A04130, the ultimate strength was 180 MPa and 176 MPa in the horizontal and vertical directions, respectively, with the ductility of about 6–8%. The obtained results are at the cast alloy A04130 level, which is acceptable but significantly lower than for similar material produced by selective laser melting (SLM) [20]. The ultimate strength of additively produced samples of AA5056 alloy was 215 MPa and 176 MPa in a horizontal and vertical direction, respectively, which is 30–40% lower than values of AA5056 alloy in the rolled state and corresponds to properties of similar cast alloys. Moreover, the ductility of additive alloy in this case is about 8–11%. The fact that the A04130 alloy is mainly used in the cast state testifies to the acceptability of its mechanical properties, but the AA5056 alloy is mainly used following sheet rolling and other methods of shaping by plastic deformation, but in this state, its properties are relatively low.

The use of FSP allowed a significant increase in the characteristics of the materials. The tensile strength of specimens cut from the stir zone increases for both alloys in horizontal and vertical directions. For the A04130 alloy in the vertical direction, the ultimate tensile strength increases with each subsequent pass until it slightly decreases on the fourth pass (Figure 8a). Its maximum value obtained with three passes is 217 MPa, and the relative elongation decreases from 17.5% (1 pass) to 15.1% (3 passes). In the horizontal direction, the maximum strength was observed at three passes and the minimum at two passes and was 207 MPa and 196 MPa, respectively (Figure 8b). For both cases of additively manufactured A04130 samples, the processing increased the metal strength by 12–15%, while the ductility remained at the same level. If to compare this result with friction welding of similar material made by SLM, the initial structure of EBAM'ed material provides initially lower

strength. Whereas, at SLM, the ultimate tensile strength of as-built material is higher almost by two times [21]. The application of friction welding to SLM material increases the size of structural elements and decreases material strength. In contrast, the application of FSP to EBAM'ed material provides a decrease in the size of structural elements and the formation of a fine-grained structure. It concludes that for EBAM'ed Al-Si alloys, friction stir processing is more preferable to the same treatment for SLM'ed materials.
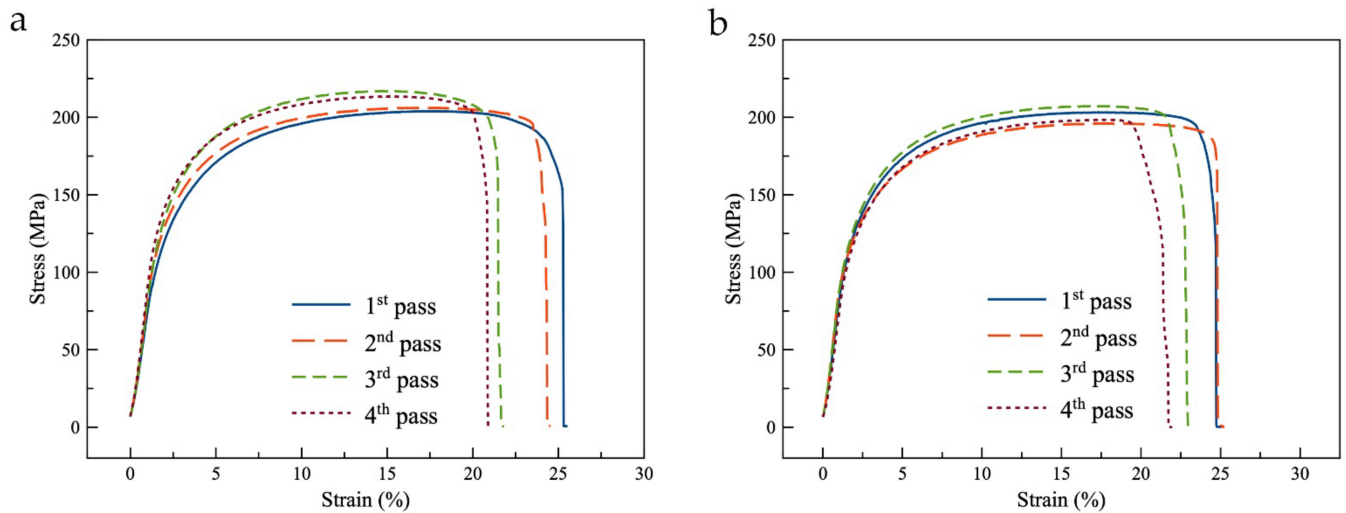

Figure 8. Tensile test diagrams of A04130 alloy specimens after FSP in vertical (**a**) and horizontal (**b**) directions.

For AA5056 alloy processed in the vertical direction, the maximum value of the ultimate tensile strength of the stir zone was observed at 2 and 3 passes (329 MPa), and the minimum at four pass (267 MPa), with the relative elongation increasing with each subsequent pass (Figure 9a). The strength decrease at multipass FSP is also noted in some works and is associated with the stir zone structural changes [22]. The highest strength was observed in the horizontal direction at third and fourth passes (311–312 MPa), and the ductility at three passes is 17% (Figure 9b). When processed in both directions, the strength properties of AA5056 alloy increase to values exceeding the strength properties of rolled sheets of the corresponding alloy. In this case, if in the ultimate strength such excess is slight, then in the ductility, such excess can reach more than 1.6 times.
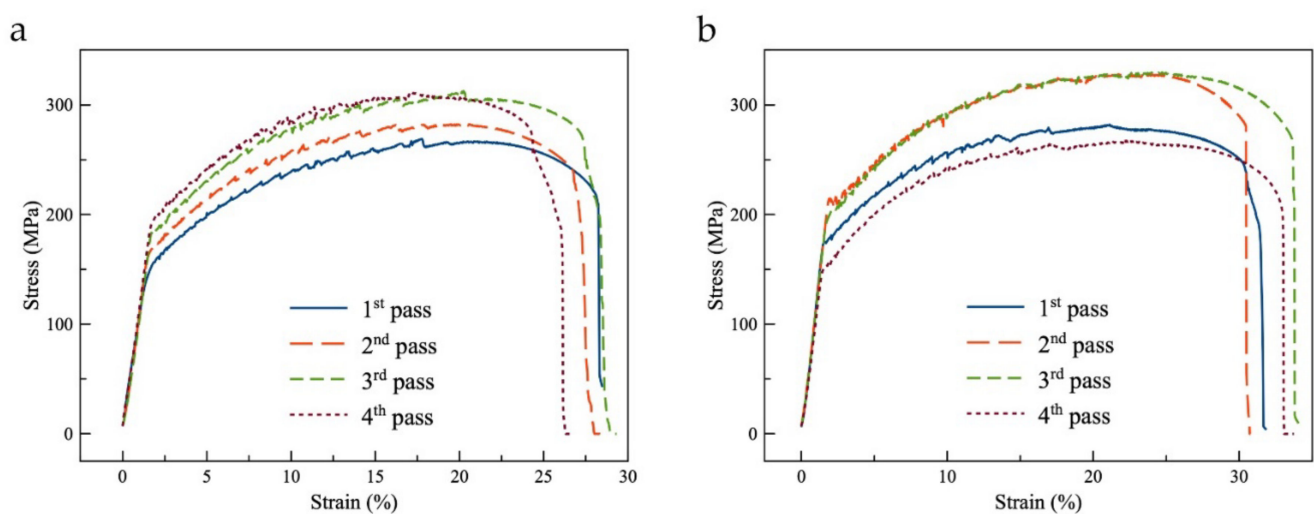

Figure 9. Tensile test diagrams of specimens after FSP of AA5056 alloy in vertical (**a**) and horizontal (**b**) directions.

Microhardness profiles for A04130 alloy produced for the first and fourth passes of the samples in vertical and horizontal directions show more uniform microhardness values in the stir zone than the base metal (Figure 10). The highest values are presented in the vertical FSP direction, both for the first and fourth passes. As a whole, it is possible to allocate only minor microhardness changes in the stir zone after 1–4 passes by the tool along a processing line.
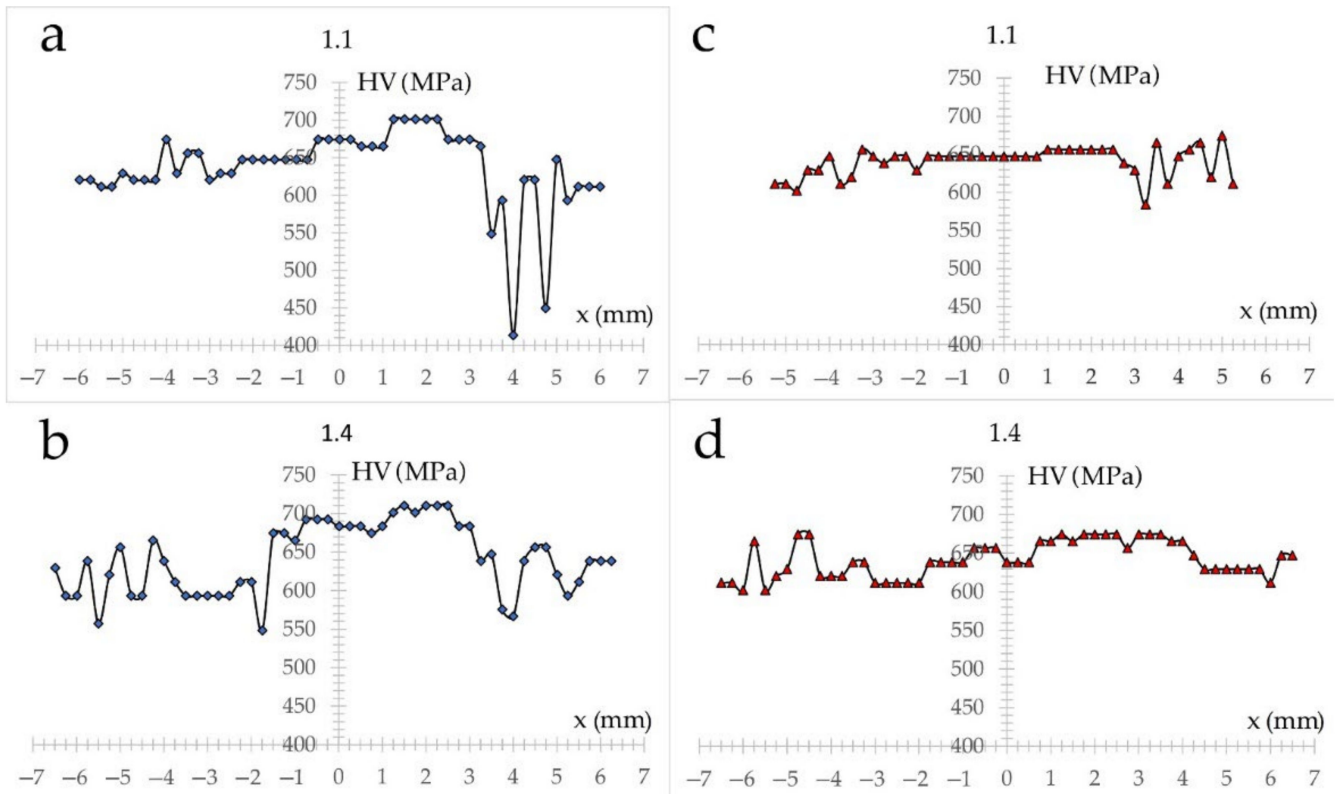
Figure 10. Distribution of microhardness values in A04130 alloy samples after FSP in vertical (**a,b**) and horizontal (**c,d**) directions. HV—Vickers hardness.

Measurements of microhardness values for alloy AA5056 after FSP received for the first and fourth passes of samples in vertical (Figure 11a,b) and horizontal (Figure 11c,d) directions show an increase of values in the stir zone in comparison with the base metal. There is a significant increase in microhardness after four passes in both cases. A more uniform change in values is observed in the SZ for the first pass measurements in both directions. However, the micro-hardness values at the fourth pass are significantly higher than those after the first one. The higher microhardness values in the stir zone can be explained by the change in the grain size relative to the base metal and by the refinement of the inclusions of secondary particles of the strengthening phases.
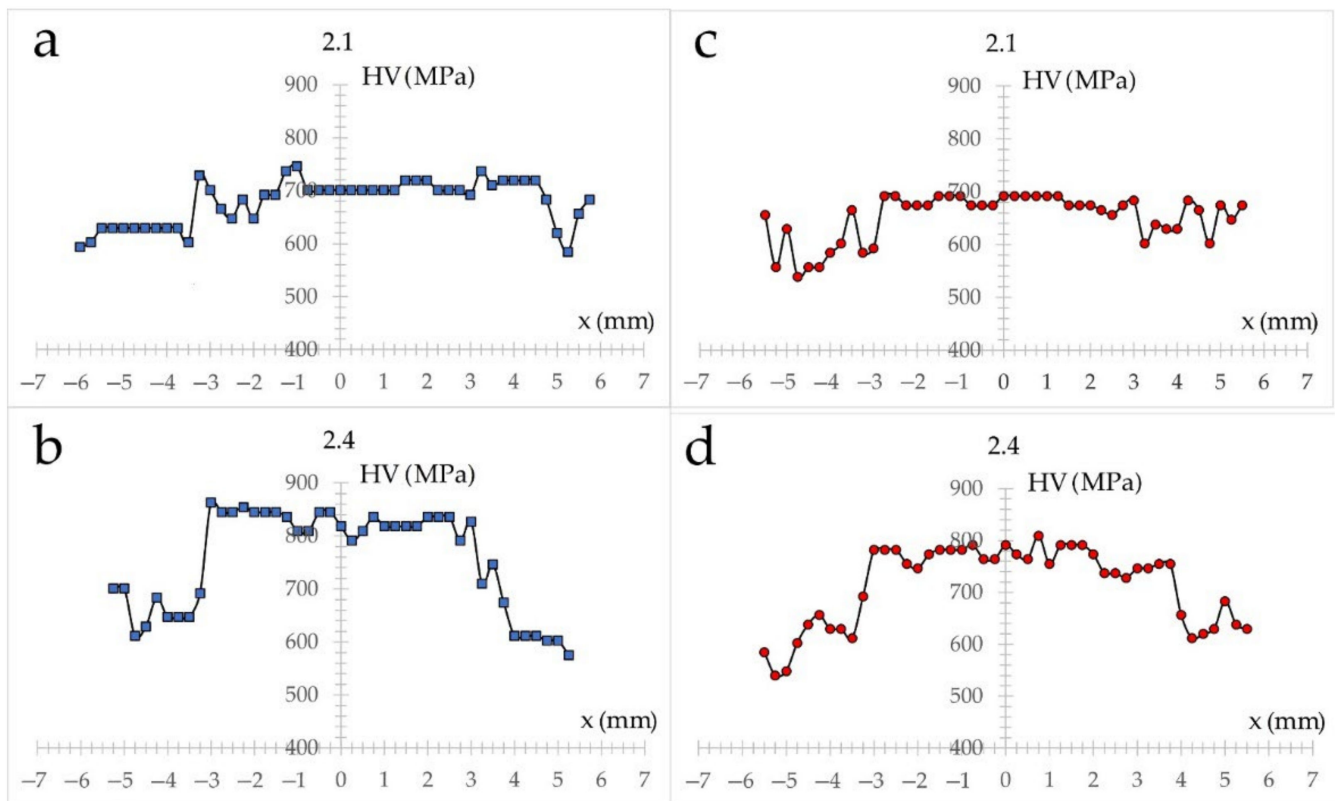
Figure 11. Distribution of microhardness values in AA5056 alloy samples after FSP in vertical (**a**,**b**) and horizontal (**c**,**d**) directions. HV—Vickers hardness.

4. Discussion

Therefore, it is evident from the data obtained that friction stir processing positively affects the properties of additively fabricated aluminum alloys. However, to achieve the maximum hardening effect from the FSP application, it is necessary to focus on the processing direction. The A04130 alloy shows better properties when processed horizontally, i.e., in the additive layer deposition direction, whereas the same is true for the AA5056 alloy in the additive growth direction (vertical). The reason for this material behavior is the structure of the original metal. Because the structure of AA5056 aluminum alloy is represented by large columnar grains whose epitaxial growth is directed in the vertical axis, the material resistance to tool movement is higher when processing in the horizontal direction than in the vertical one (a similar effect was obtained in [23]). In turn, the A04130 alloy in the as-built state is represented by a dendritic structure (i.e., no grain boundaries), making it easier to pass the tool in the horizontal direction and resulting in increased material properties. However, despite this effect of additive workpiece structure, material hardening relative to the base metal occurs regardless of the processing direction. Such mechanical properties improvements caused by the material undergo dynamic recrystallization during processing. As a result, a fine-grained structure is formed in the stir zone, regardless of whether the material is dendritic or coarse-grained. With subsequent passes, both the material's ultimate strength and microhardness are increased up to the third pass. Nevertheless, the authors of work [22] note that an increase in passes number is accompanied by an increase in the stir zone grain size, which leads to the strength decrease in most cases. In this work, a similar effect is observed starting from the fourth pass. However, the obtained tensile strength values are still higher than the base material ones. Moreover, to consider multipass processing as a way to form composite materials by the FSP method, grain growth in the stir zone with multiple passes will be limited by adding strengthening particles to the processing area and creating additional crystallization centers [24]. One makes it possible to apply friction stir processing to various types of aluminum alloys produced by additive

manufacturing methods, particularly wire-feed electron beam additive manufacturing, both for local material hardening and for creating metal-matrix composites.

5. Conclusions

As a result of these studies, it was found that the effect of friction stir processing and the number of passes on products made of aluminum-silicon alloy A04130 and aluminum-magnesium alloy AA5056, manufactured by electron beam additive technology, is different. Metal hardening exceeds tabulated values for sheet AA5056 and cast A04130 alloy without significantly reducing ductility. The most significant effect on mechanical properties was achieved in the processing of alloy AA5056, for which the tensile strength increase, although significant, was inferior to the increase in the ductility up to 1.6 times. The initial structure of additive alloys influences the choice of processing direction. In the case of columnar grain formation, when processing in the horizontal direction, the strength of the stir zone material decreases due to the increased resistance of the material to the tool movement.

Based on the results obtained, it can be concluded that for the aluminum-magnesium alloy, the FSP is suitable and has a positive effect on the product quality. At the same time, despite the high performance, the FSP is not necessary for the A04130 alloy, as additively manufactured products are already superior to cast products. Nevertheless, this processing can still be applicable for forming composites based on aluminum-silicon alloys.

References

1. Summer, F.; Pusterhofer, M.; Grün, F.; Gódor, I. Tribological investigations with near eutectic AlSi alloys found in engine vane pumps—Characterization of the material tribo-functionalities. *Tribol. Int.* **2020**, *146*, 106236. [CrossRef]
2. Stempera, L.; Tunes, M.A.; Tosone, R.; Uggowitzer, P.J.; Pogatscher, S. On the potential of aluminum crossover alloys. *Prog. Mater. Sci.* **2022**, *124*, 100873. [CrossRef]
3. Zhang, G.; Xiong, H.; Yu, H.; Qin, R.; Liu, W.; Yuan, H. Microstructure evolution and mechanical properties of wire-feed electron beam additive manufactured Ti-5Al-2Sn-2Zr-4Mo-4Cr alloy with different subtransus heat treatments. *Mater. Des.* **2020**, *195*, 109063. [CrossRef]
4. Kalashnikov, K.N.; Rubtsov, V.E.; Savchenko, N.L.; Kalashnikova, T.A.; Osipovich, K.S.; Eliseev, A.A.; Chumaevskii, A.V. The effect of wire feed geometry on electron beam freeform 3D printing of complex-shaped samples from Ti-6Al-4V alloy. *Int. J. Adv. Manuf. Technol.* **2019**, *105*, 3147–3156. [CrossRef]
5. Astafurov, S.; Astafurova, E.; Reunova, K.; Melnikov, E.; Panchenko, M.; Moskvina, V.; Maier, G.; Rubtsov, V.; Kolubaev, E. Electron-beam additive manufacturing of high-nitrogen steel: Microstructure and tensile properties. *Mater. Sci. Eng. A* **2021**, *826*, 141951. [CrossRef]
6. Liu, Y.; Zhang, J.; Tan, Q.; Yin, Y.; Liu, S.; Li, M.; Li, M.; Liu, Q.; Zhou, Y.; Wu, T.; et al. Additive manufacturing of high strength copper alloy with heterogeneous grain structure through laser powder bed fusion. *Acta Mater.* **2021**, *220*, 117311. [CrossRef]
7. Kotadia, H.; Gibbons, G.; Das, A.; Howes, P. A review of Laser Powder Bed Fusion Additive Manufacturing of aluminium alloys: Microstructure and properties. *Addit. Manuf.* **2021**, *46*, 102155. [CrossRef]
8. Lathabai, S. Chapter 2—Additive Manufacturing of Aluminium-Based Alloys and Composites. In *Woodhead Publishing Series in Metals and Surface Engineering: Fundamentals of Aluminium Metallurgy, Recent Advances*; Lumley, R.N., Ed.; Woodhead Publishing: Duxford, UK, 2018; pp. 47–92. ISBN 978-0-08-102063-0.
9. Zykova, A.; Chumaevskii, A.; Vorontsov, A.; Kalashnikov, K.; Gurianov, D.; Gusarova, A.; Kolubaev, E. Evolution of microstructure and properties of Fe-Cu, manufactured by electron beam additive manufacturing with subsequent friction stir processing. *Mater. Lett.* **2021**, *307*, 131023. [CrossRef]

10. Nasiri, Z.; Khorrami, M.S.; Mirzadeh, H.; Emamy, M. Enhanced mechanical properties of as-cast Mg-Al-Ca magnesium alloys by friction stir processing. *Mater. Lett.* **2021**, *296*, 129880. [CrossRef]

11. El-Sayed, M.M.; Shash, A.; Abd-Rabou, M.; ElSherbiny, M.G. Welding and processing of metallic materials by using friction stir technique: A review. *J. Adv. Join. Process.* **2021**, *3*, 100059. [CrossRef]

12. Mehta, K.; Badheka, V. Wear behavior of boron-carbide reinforced aluminum surface composites fabricated by Friction Stir Processing. *Wear* **2019**, *426–427*, 975–980. [CrossRef]

13. Singh, A.K.; Ratrey, P.; Astarita, A.; Franchitti, S.; Mishra, A.; Arora, A. Enhanced cytocompatibility and mechanical properties of electron beam melted Ti-6Al-4V by friction stir processing. *J. Manuf. Process.* **2021**, *72*, 400–410. [CrossRef]

14. Mehdi, H.; Mishra, R. Effect of multi-pass friction stir processing and SiC nanoparticles on microstructure and mechanical properties of AA6082-T6. *Adv. Ind. Manuf. Eng.* **2021**, *3*, 100062. [CrossRef]

15. Chen, Y.; Cai, Z.; Ding, H.; Zhang, F. The Evolution of the Nugget Zone for Dissimilar AA6061/AA7075 Joints Fabricated via Multiple-Pass Friction Stir Welding. *Metals* **2021**, *11*, 1506. [CrossRef]

16. Estrin, Y.; Vinogradov, A. Fatigue behaviour of light alloys with ultrafine grain structure produced by severe plastic de-formation: An overview. *Int. J. Fatigue* **2010**, *32*, 898–907. [CrossRef]

17. Zykova, A.; Chumaevskii, A.; Gusarova, A.; Gurianov, D.; Kalashnikova, T.; Savchenko, N.; Kolubaev, E.; Tarasov, S. Evolution of Microstructure in Friction Stir Processed Dissimilar CuZn37/AA5056 Stir Zone. *Materials* **2021**, *14*, 5208. [CrossRef] [PubMed]

18. Zykova, A.P.; Tarasov, S.Y.; Chumaevskiy, A.V.; Kolubaev, E.A. A Review of Friction Stir Processing of Structural Metallic Materials: Process, Properties, and Methods. *Metals* **2020**, *10*, 772. [CrossRef]

19. Krishnan, K. On the formation of onion rings in friction stir welds. *Mater. Sci. Eng. A* **2002**, *327*, 246–251. [CrossRef]

20. Suryawanshi, J.; Prashanth, K.; Scudino, S.; Eckert, J.; Prakash, O.; Ramamurty, U. Simultaneous enhancements of strength and toughness in an Al-12Si alloy synthesized using selective laser melting. *Acta Mater.* **2016**, *115*, 285–294. [CrossRef]

21. Prashanth, K.; Damodaram, R.; Scudino, S.; Wang, Z.; Rao, K.P.; Eckert, J. Friction welding of Al–12Si parts produced by selective laser melting. *Mater. Des.* **2014**, *57*, 632–637. [CrossRef]

22. Ramesh, K.N.; Pradeep, S.; Pancholi, V. Multipass Friction-Stir Processing and its Effect on Mechanical Properties of Aluminum Alloy 5086. *Met. Mater. Trans. A* **2012**, *43*, 4311–4319. [CrossRef]

23. Kalashnikova, T.A.; Chumaevskii, A.V.; Rubtsov, V.E.; Kalashnikov, K.N.; Kolubaev, E.A.; Eliseev, A.A. Structural Heredity of the Aluminum Alloy Obtained by the Additive Method and Modified Under Severe Thermomechanical Action on Its Final Structure and Properties. *Russ. Phys. J.* **2020**, *62*, 1565–1572. [CrossRef]

24. Sharma, V.; Prakash, U.; Kumar, B.M. Surface composites by friction stir processing: A review. *J. Mater. Process. Technol.* **2015**, *224*, 117–134. [CrossRef]